of Oxygen, Nitrogen, Carbon Monoxide and Their Binary Mixtures on Molecular Sieve Type 10X," *J. Chem. Eng. Data*, **26**, 112 (1981).
Suwanayuen, S., and R. P. Danner, "A Gas Adsorption Isotherm Equation Based on Vacancy Solution Theory," *AIChE J.*, **26**, 68 (1980a).
Suwanayuen, S., and R. P. Danner, "Vacancy Solution Theory of Adsorption from Gas Mixtures," *AIChE J.*, **26**, 76 (1980b).
Szepesy, L. and V. Illés, "Adsorption of Gases and Gas Mixtures. I: Measurement of the Adsorption Isotherms of Gases on Activated Carbon up to Pressures of 1000 torr.," *Acta. Chim. Hung.*, **35**, 37 (1963a).
——, "Adsorption of Gases and Gas Mixtures. II: Measurement of the Adsorption Isotherms of Gases on Activated Carbon under Pressures of 1 to 7 atm.," *Acta. Chim. Hung.*, **35**, 53 (1963b).
——, "Adsorption of Gases and Gas Mixtures. III: Investigation of the Adsorption Equilibria of Binary Gas Mixtures," *Acta. Chim. Hung.*, **35**, 245 (1963c).
Wilson, R. J., and R. P. Danner, "Adsorption of Synthesis Gas-Mixture Components on Activated Carbon," *J. Chem. Eng. Data*, **28**, 14 (1983).

Manuscript received August 2, 1983; revision received January 5, 1984, and accepted January 12.

Longitudinal and Lateral Dispersion in Packed Beds: Effect of Column Length and Particle Size Distribution

Longitudinal and lateral dispersion coefficients were measured at various axial positions in a packed bed in the Peclet number range from 10^2 to 10^4. Three different types of packings were used: uniform size particles, a narrow size distribution, and a wide size distribution. For the case of uniform particles the longitudinal dispersivities were found to be strong functions of position in the bed unless the dispersion length satisfies a constraint dependent on the value of the Peclet number. Generally, the larger the Peclet number, the larger the required length for constant axial dispersivities to be achieved. For the case of the wide size distribution, longitudinal dispersivities were larger than in the uniform particle case, and they required a longer dispersion length to achieve a constant value. This suggests a characteristic length for dispersion larger than the mean hydraulic radius. The lateral dispersivities were found to be insensitive to the distribution of particle sizes or location in the bed.

NEUNG-WON HAN, JAYENDRA BHAKTA, and R. G. CARBONELL

Department of Chemical Engineering
North Carolina State University
Raleigh, NC 27695

SCOPE

The dispersion equation is used to calculate the average concentration of a solute in a porous medium under flow conditions (Bear, 1972; Dullien, 1979). The dispersive term accounts for the spread of the solute about the mean pulse position due to molecular diffusion and the coupling of interparticle velocity and concentration gradients (Whitaker, 1967; Gray, 1975). It consists of the double scalar product of a dispersion tensor, or total dispersivity tensor (Brenner, 1980) with the second derivative of the average solute concentration in the porous medium. For the case of an isotropic porous medium, the total dispersivity tensor has non-zero components only along the diagonal. The diagonal element corresponding to the mean direction of flow is called the longitudinal dispersion coefficient and it contributes to the spread of solute pulses along the flow direction. The other on-diagonal elements are called the lateral dispersion coefficients and they contribute to the spread of the solute in the directions orthogonal to the mean flow.

There have been many experimental measurements of the longitudinal dispersion coefficient in packed beds and its dependence on the Peclet number (Harleman and Rumer, 1963; Edwards and Richardson, 1968; Rifai et al., 1956; Carberry and Bretton, 1958; Ebach and White, 1958; Pfannkuch, 1963; Blackwell et al., 1959; Gunn and Pryce, 1969). The Peclet number dependence of the lateral dispersion coefficient has not been measured as extensively but there are some data at low Peclet numbers (Harleman and Rumer, 1963; Gunn and Pryce, 1969; Grane and Gardner, 1961; Hassinger and von Rosenberg, 1968; Blackwell, 1962). Implicit in these studies is the assumption that the dispersion coefficients are constants that depend on the value of the Reynolds and Schmidt numbers only, and are independent of position in the packed bed or porous medium. However, G. I. Taylor (1953, 1954) in his original work on dispersion in capillary tubes was very careful to point out that dispersion models become valid only after a sufficiently long time has passed since the insertion of the solute pulse. How long this time is in a particular experiment was shown to depend on the value of the molecular diffusivity, the tube radius, and the average fluid velocity. More recently, Brenner (1980) showed that dispersion models are valid asymptotically in time for the case of dispersion in spatially periodic porous media, while

Correspondence concerning this paper should be addressed to R. G. Carbonell.
Neung-won Han is presently at the Department of Chemical Engineering, Chon-nam National University, Kwang-ju, Korea.
Work done while authors were in the Chemical Engineering Department, University of California, Davis.

Carbonell and Whitaker (1983) demonstrated that this should be the case for any porous medium. Unfortunately, in the design of most dispersion experiments in packed beds this possible dependence of the dispersion coefficient on time was not investigated. The first objective of this work is to measure the axial dispersion coefficient at various axial positions in a packed bed, for a fairly wide range of Peclet numbers. At very low flow rates, the experiments last a sufficiently long time so that the asymptotic value of the dispersion coefficient can develop. This would be reflected in a constant value of the axial dispersivity at various positions along the column length. At very high flow rates the experiments take a very short time and the dispersion coefficient should be a function of axial position in the column. By analyzing these results, a quantitative criterion can be developed for the time required for the dispersion coefficient to become constant.

Most experiments on dispersion coefficients, both longitudinal and lateral, have been carried out with particles with a very narrow size distribution. There has been little systematic effort to determine the effect of particle size distribution on dispersion coefficients. This information would be of use to workers interested in applying dispersion models to problems in transport processes in soils, coal gasification, or oil shale retorting, for example, where there are fairly large distributions of particle sizes. Carbonell (1979; 1980a,b) has made some preliminary estimates of the effect of particle size distribution on dispersion using a capillary tube model for the porous medium. However, with the exception of some early work of Niemann (1969), little experimental information is available on how particle size distributions affect dispersion coefficients. The second objective of this study is to vary systematically the distribution of particle sizes in a packed bed and to study the effect of this change in porous medium structure on the magnitude of the longitudinal and lateral dispersion coefficients.

The data on lateral dispersion coefficients in packed beds has been limited in previous studies to particle Peclet numbers less than 10^3. The third objective of our work was to extend the range of available values of lateral dispersivities to particle Peclet number of 10^4 or greater. Both longitudinal and lateral dispersion coefficients were measured in the Peclet number range of 10^2 to 10^4.

CONCLUSIONS AND SIGNIFICANCE

It was found that the longitudinal dispersivities for uniform size packings are a function of position in the bed unless the approximate criterion

$$\left(\frac{L}{d_p}\right)\frac{1}{Pe_p}\left(\frac{1-\epsilon}{\epsilon}\right) \geq 0.3$$

is satisfied. For very high Peclet numbers, one needs a larger ratio of bed length to particle diameter in order to treat the longitudinal dispersivity as a constant. If the criterion above is not satisfied, one observes significantly lower values of axial dispersion coefficients that depend strongly on bed location. Some of the previous results in the literature indicate that the longitudinal dispersivity depends less strongly on the Peclet number at very high values of Pe_p than at lower values. This has been attributed to turbulence effects. However, a similar phenomenon is observed in this work under laminar flow conditions when the dispersion distances are too short to satisfy the constraint above. At least some of the curvature of previous data is believed to have resulted from this effect.

Lateral dispersivities were measured using a steady-state experiment over a Peclet number range of 10^2 to 10^4. This extended the range of available lateral dispersion data which previously had been limited to a Peclet number of 10^3. No dependence of the lateral dispersivity on bed location was observed.

The effect of particle size distribution on longitudinal and lateral dispersivities was studied by making up two size distributions that had the same mean particle diameter and volume fraction that was used in the experiments for uniform size particles. The first size distribution had a ratio of maximum to minimum particle diameter of 2.2, the second size distribution had a corresponding ratio of 7.3. The longitudinal dispersivities for the uniform particle size and the first size distribution were nearly identical. The second size distribution exhibited longitudinal dispersivities 2 to 3 times larger than the uniform size particles. It was also observed that the bed length required to reach a constant value of the longitudinal dispersivity was much longer in the case of size distribution 2 than the case of uniform particles. Both of these results indicate that the characteristic length for longitudinal dispersion for the case of nonuniform particle size distributions is much longer than the hydraulic radius of the packing. This suggests the presence of larger scale nonuniformities that strongly influence the longitudinal dispersion behavior. At the present time there is not enough data to provide a quantitative measure of the size of this length scale, or how it correlates with the width of the particle size distribution. The lateral dispersivities, which were measured under steady state conditions, showed no dependence on the particle size distribution.

INTRODUCTION

Since the development of the dispersion approximation for the study of solute transport in capillary tubes by G. I. Taylor (1953, 1954) and R. Aris (1956), a great deal of work has been done in applying these principles to the description of solute transport in porous media such as soils and packed bed reactors (Dullien, 1979; Bear, 1972). By using the method of volume or spatial averaging (Slattery, 1972) it is possible to derive the proper form of the transport equation for the average concentration of solute in a porous medium (Whitaker, 1967; Gray, 1975; Bear, 1972). Carbonell and Whitaker (1983) and Brenner (1980) have shown that for the case of spatially periodic models of porous media, one can have a predictive theory that can be used to calculate values of the dispersion coefficients without any adjustable parameters. Eidsath et al. (1983) have computed axial and lateral dispersion coefficients in packed beds based on these spatially periodic models, and have compared the results to available experimental data. Of course, in soils or underground reservoirs, large scale nonuniformities can lead to much different values of dispersion coefficients than those measured in packed beds, and for these cases spatially periodic models cannot be expected to provide excellent results without modifications. There have been other attempts at correlating and predicting dispersion coefficients based on a probabilistic approach (Greenkorn and Kessler, 1970; Haring and Greenkorn, 1970; Saffman, 1967; De Josselin de Jong, 1958) where the network of pores in the porous medium is regarded as an array of cylindrical capillaries with radii, lengths, and angular orientations governed by probability distribution functions. The agreement of these models with experimental data is not complete. For example, the spatially periodic models studies so far tend to overestimate the Peclet number dependence of axial dispersion coefficients and grossly underestimate the magnitude and Peclet number dependence of lateral dispersivities. The probabilistic models have many

adjustable parameters, and it is difficult to predict a priori what values of the parameters should be used to represent accurately the dispersion behavior in a given porous medium. In addition to improved theoretical and computational efforts, it is important to have an expanded data base of dispersion coefficients which can be used to clarify and support theoretical developments and improve our understanding of the relationship between the structure of the porous medium and its dispersive properties. In this paper we focus attention on three aspects of solute dispersion which have not been carefully examined. The first is the possible dependence of the axial dispersion coefficient on position in a packed bed. The second is the effect of the distribution of particle sizes on longitudinal and lateral dispersion coefficients, and the third is the Peclet number dependence of the lateral dispersivity.

From the form of the exact solution to the convective-diffusion equation in laminar flow in a capillary tube, Taylor (1953, 1954) was able to argue quite effectively that the dispersion approximation would be valid for times t after the pulse injection such that the following constraint is satisfied

$$\theta = \frac{\mathcal{D}t}{R^2} \gg 0.14 \tag{1}$$

Here θ is a dimensionless time, R is the tube radius, and $\mathcal{D}$ is the molecular diffusivity of the solute in the fluid. Gill and Sankarasubramanian (1970) showed that for times shorter than those indicated by Eq. 1 the dispersion coefficient is an increasing function of time that reaches the final Taylor-Aris dispersion value asymptotically. By the time $\theta = 1$, the dispersion coefficient is within less than 1% of its asymptotic value. However, when $\theta = 0.01$, the dispersion coefficient is nearly a factor of 10 lower than its final value. Paine et al. (1983) obtained similar results using the spatial averaging technique for the case of passive dispersion, and studied the behavior of transient dispersion coefficients in laminar flow in tubes under conditions of adsorption and reaction at the tube wall. Carbonell and Whitaker (1983) concluded that even in the case of a general three-dimensional porous medium, the dispersion coefficient becomes constant subject to a constraint similar to that for a capillary tube

$$\theta = \frac{\mathcal{D}t}{l_\beta^2} \gg 1 \tag{2}$$

where l_β is a characteristic length associated with the pore spaces in the fluid-solid system. Brenner (1980) was able to prove that this is the case exactly for a spatially periodic porous medium, using a random motion approach to study the solute transport.

Even though there is a great deal of evidence acquired from theoretical analyses that the dispersion coefficients are not constant unless a constraint of the type shown in Eq. 2 is satisfied, there are no experimental data to verify these results for real porous media. In principle there can be a serious error in measured values of dispersion coefficients in packed beds if the constraint of Eq. 2 is not satisfied. This can be seen clearly if we allow l_β in Eq. 2 to be the characteristic length of pores in a bed filled with particles of diameter d_p and void fraction ϵ (Whitaker, 1972)

$$l_\beta = d_p \left(\frac{\epsilon}{1-\epsilon}\right). \tag{3}$$

If the distance from the inlet is L, and the interstitial velocity is $\langle v\rangle^\beta$, the characteristic time for a dispersion experiment becomes $L/\langle v\rangle^\beta$. Substituting these expressions in Eq. 2, we see that we cannot expect the dispersion coefficient in a packed bed to be a constant unless the ratio of the distance from the inlet to the particle diameter is related to the Peclet number by

$$\frac{L}{d_p} \gg Pe_p \left(\frac{\epsilon}{1-\epsilon}\right) \tag{4}$$

where

$$Pe_p = \frac{\langle v\rangle^\beta d_p}{\mathcal{D}} \left(\frac{\epsilon}{1-\epsilon}\right). \tag{5}$$

This is a Peclet number based on l_β in Eq. 3 as the characteristic length (Whitaker, 1972). For large Peclet numbers this constraint can become very difficult to satisfy in a column of finite length. In Table 1 we have summarized some of the experimental efforts aimed at studying the Peclet number dependence of the axial dispersivity. We have listed the experimental conditions as reported by the authors and calculated values of L/d_p and $Pe_p(\epsilon/1-\epsilon)$ for each work.

The value of L listed in Table 1 is the *largest* of all the column lengths used by the investigators if they used more than one packing length. The values of d_p are equivalent sphere diameters as some of the experiments involved non-spherical particles such as Raschig rings and cylinders. All volume fractions, fluid velocities, and particle sizes used in Table 1 came directly from the published articles. The Reynolds and Schmidt numbers were computed by estimating physical properties of the fluids used when not given explicitly in the references. To get the smallest value of Re_p for a given experiment we used the smallest velocity and particle diameter in Table 1, while the largest Re_p was computed using the largest velocity and particle diameter. The characteristic length used in the definition of Re_p is the quantity l_β defined by Eq. 3. It is clear from this summary that in several of these previous studies the criterion expressed by Eq. 4 is either marginally satisfied, or not satisfied at all. This is especially true of the experiments of

TABLE 1. SOME PREVIOUS EXPERIMENTAL MEASUREMENTS OF LONGITUDINAL DISPERSION COEFFICIENTS

Authors	Solvent	Solute	L (cm)	d_p (cm)	ϵ	$\langle v\rangle^\beta$ (cm/s)	Re_p	Sc	L/d_p	$Pe_p\frac{\epsilon}{1-\epsilon}$
1. Harleman and Rumer (1963)	Water	NaCl	273.5	0.096	0.36	0.00608–0.130	0.035–21.4	560	2,849	11.02–6,741
2. Edwards and Richardson (1968)	Air	Argon	100.0	0.0377–0.607	0.361–0.420	0.0903–32.3	0.0133–96.1	0.72	2,652–165	0.0053–50.1
3. Rifai et al. (1956)	Water	NaCl	127.0	0.025–0.045	0.375–0.395	0.0005–0.1600	0.000807–0.506	560	5,080–2,822	0.452–185
4. Carberry and Bretton (1958)	Water	Dye	61.3	0.05–0.6	0.365–0.645	0.09–23	0.258–2144	1,858	1,226–102	276–7.24 × 10^6
5. Ebach and White (1958)	Water	Dye	152.4	0.021–0.673	0.34–0.632	0.0236–8.22	0.0275–1023	1,858	7,257–226.4	26.3–3.26 × 10^6
6. Pfannkuch (1963)	Water	NaCl	150.0	0.0355–0.21	0.34–0.388	0.00035–0.6639	0.00069–9.59	560	4,225–714	0.199–3,405
7. Blackwell et al. (1959)	Argon	Helium	3,658.0	0.021	0.339	0.023–0.72	0.00298–0.200	1.82	1.74 × 10^5	0.0028–0.188
8. Gunn and Pryce (1969)	Air	Argon	26.5	0.037–0.6	0.37	1.8–117	0.234–246.6	0.88	716.2–44.2	0.120–127.4

Carberry and Bretton (1958) and Ebach and White (1958), where extremely large values of the Peclet number were reached, as well as those of Pfannkuch (1963) where the L/d_p ratio in some cases was significantly smaller than the Peclet number. Harleman and Rumer (1963) used a packed bed with one probe at the inlet and two other probes downstream, but did not mention any effect of the probe location on the measured axial dispersion coefficients. Rifai et al. (1956) also measured axial dispersivities at several locations in the bed and found no effect, but their experiments satisfy the length criterion in Eq. 4 throughout the entire range of Peclet numbers. Carberry and Bretton (1958) found that the longitudinal dispersion coefficient decreased with bed height, but they correctly ascribed this to a flow redistribution problem in their experiment. Ebach and White (1958) and Pfannkuch (1963) mention that three different column lengths were used in their experiments but apparently they did not make a systematic effort to study the effect of column length on the measured values of the dispersivity. In this paper we provide data on longitudinal dispersivities as a function of axial position in a packed bed for Peclet numbers ranging from 10^2 to 10^4. This information is of fundamental importance in understanding some of the data acquired on longitudinal dispersion, especially in those experiments where the ratio of L/d_p does not satisfy the criterion of Eq. 4. It should also be of a practical interest, since in the design of packed beds for catalytic reactors and other applications it is often very difficult to achieve very large ratios of column length to particle diameter.

Another aspect of dispersion in packed beds and porous media in general that has not received systematic attention is the effect of the porous medium structure on total dispersivity. Of recent interest has been the effect of particle size distribution on longitudinal and lateral dispersion coefficients. This information is necessary in attempts to model solute transport in soils as well as in reactors for shale oil retorting and coal gasification and liquefaction (Carbonell, 1979; 1980a,b). With the single exception of some work by Niemann (1969), no workers in the field have varied the width of the distribution of particle sizes in a packed bed and then examined the effects on longitudinal and lateral dispersion. Eidsath et al. (1983) performed some calculations on spatially periodic arrays of staggered cylinders of two different radii that indicated a strong effect of particle size distribution on dispersion. As the ratio of the cylinder radii went from a value of 2 to 5, the axial dispersion coefficient increased by a factor of 1.5. In contrast, the lateral dispersion coefficient decreased by about the same amount. It would be of interest to see to what extent this phenomenon would be observed in a real porous medium, since it would provide some insight into how one might apply axial dispersion data taken in beds of uniform particles to systems with highly nonuniform particle size distributions. In this paper we report some observations made on the way that longitudinal and lateral dispersion coefficients vary as the width of the particle size distribution is increased, but the mean particle diameter and volume fraction remain the same, for the Peclet number range from 10^2 to 10^4.

The lateral dispersion coefficients are the most difficult components of the total dispersivity tensor to measure since they require a technique for measuring concentration profiles in a packed bed in a direction normal to the flow direction under either transient or steady-state conditions. The most accurate experiments have been done by Harleman and Rumer (1963), in which they covered the particle Peclet number range from 10 to 10^3. Hassinger and von Rosenberg (1968) measured lateral dispersion coefficients at lower Peclet numbers from 10^{-1} to 10^2, while Gunn and Pryce (1969) covered the same Peclet number range as Harleman and Rumer (1963) but obtained a considerably higher Peclet number dependence on the lateral dispersivity. The theoretical models of Brenner (1979) and Carbonell and Whitaker (1982) for spatially periodic porous media allow a priori predictions of lateral dispersivities. However, a very firm data base is not available for comparison with experimental data. In this investigation we studied the Peclet number dependence of lateral dispersion coefficients up to a value of the Pe_p of about 10^4, and compare our results to previous experiments and to theoretical predictions. In the next section of this paper we present a brief summary of the theory of dispersion of inert solutes in a porous medium. This is followed by a detailed description of the experimental techniques and results as well as a comparison of all the data available on longitudinal and lateral dispersion coefficients in packed beds.

THEORY OF DISPERSION OF AN INERT SOLUTE

The volume-averaged form of the transport equation for the average concentration of solute in the fluid phase takes the form

$$\frac{\partial \langle c \rangle^\beta}{\partial t} + \langle \boldsymbol{v} \rangle^\beta \cdot \nabla \langle c \rangle^\beta = \boldsymbol{D}^* : \nabla\nabla \langle c \rangle^\beta \tag{6}$$

where $\boldsymbol{D}^*$ is the total dispersivity tensor (Carbonell and Whitaker, 1983). The total dispersivity has contributions from diffusion as well as hydrodynamic dispersion

$$\boldsymbol{D}^* = \frac{1}{2}[\mathcal{D}(\boldsymbol{I} + \boldsymbol{\tau}) + \boldsymbol{D}] + \frac{1}{2}[\mathcal{D}(\boldsymbol{I} + \boldsymbol{\tau}^T) + \boldsymbol{D}^T]. \tag{7}$$

In the equation above $\boldsymbol{\tau}$ is the tortuosity tensor

$$\boldsymbol{\tau} = \frac{1}{V_\beta} \int_{A_{\beta\sigma}} \boldsymbol{n}\boldsymbol{f} dA \tag{8}$$

and $\boldsymbol{D}$ is the hydrodynamic dispersion tensor

$$\boldsymbol{D} = -\langle \tilde{\boldsymbol{v}}\boldsymbol{f} \rangle^\beta \tag{9}$$

with the spatial deviation of the velocity from the average defined by

$$\tilde{\boldsymbol{v}} = \boldsymbol{v} - \langle \boldsymbol{v} \rangle^\beta \tag{10}$$

The vector $\boldsymbol{f}$ is a function of position that relates the local spatial deviations of the point concentration from the average value to the gradient in the average concentration

$$c - \langle c \rangle^\beta = \tilde{c} = \boldsymbol{f} \cdot \nabla \langle c \rangle^\beta \tag{11}$$

This relation is valid for a homogeneous porous medium when a sufficiently long time has passed after the introduction of the solute pulse so that the quasi-steady assumption is satisfied

$$\frac{t\mathcal{D}}{l_\beta^2} \gg 1. \tag{12}$$

This assumption makes the spatial deviation field $\tilde{c}$ quasi-steady, and this restriction is consistent with the Aris-Taylor approximation for dispersion in a capillary tube. The vector field $\boldsymbol{f}$ has been computed by Eidsath et al. (1983) for the case of a spatially periodic array of particles. This allowed a direct calculation of the tortuosity and hydrodynamic dispersion tensors. In the section that follows, we describe how one can measure the elements of the tensor $\boldsymbol{D}^*$ experimentally. However, one should keep in mind that if Eq. 12 is not satisfied, the elements of the total dispersivity tensor cannot be expected to be constant in time. This would reflect itself in different dispersivity values observed at different points in the column, even though the volume fraction is constant.

Longitudinal and Lateral Dispersivities

Let us consider an experiment where the velocity field is unidirectional

$$\langle \boldsymbol{v} \rangle^\beta = \langle v_x \rangle^\beta \boldsymbol{i}. \tag{13}$$

The coordinate system is shown in Figure 1. For the case of uniform void fraction ϵ the volume-averaged continuity equation reduces to the form

$$\nabla \cdot \langle \boldsymbol{v} \rangle^\beta = \frac{d\langle v_x \rangle^\beta}{dx} = 0 \tag{14}$$

so that the interstitial velocity remains constant along the flow direction. At the entrance to the column we introduce a time-

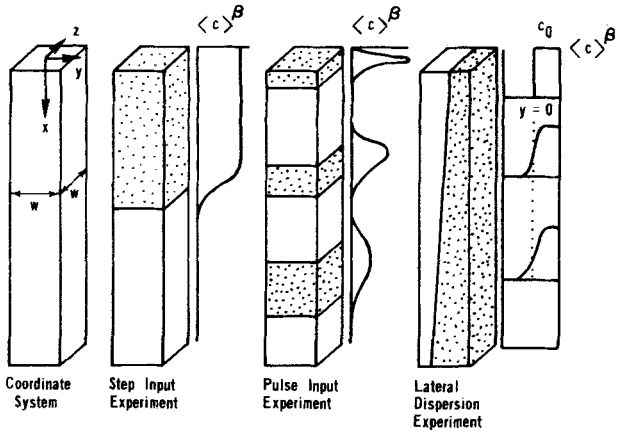

Figure 1. Coordinate system and schematic of longitudinal and lateral dispersivity experiments.

varying concentration which is independent of the directions normal to the flow direction

$$\langle c\rangle^{\beta} = F(t) \quad x = 0 \tag{15}$$

Since there is zero flux of solute in the y and z directions along the column length, Eq. 6 reduces to

$$\frac{\partial\langle c\rangle^{\beta}}{\partial t} + \langle v_x\rangle^{\beta}\frac{\partial\langle c\rangle^{\beta}}{\partial x} = D^{*}_{xx}\frac{\partial^2\langle c\rangle^{\beta}}{\partial x^2} \tag{16}$$

where D^{*}_{xx} is the longitudinal or axial dispersivity. For very long columns it is appropriate to use the boundary condition

$$\langle c\rangle^{\beta} \to 0 \quad \text{as } x \to \infty \tag{17}$$

so that the column outlet does not influence the concentration profiles in the bed. The solution to Eq. 16 subject to a step change in concentration at the bed entrance

$$\mathcal{F}(t) = c_o u(t) \quad \text{at } x = 0 \tag{18}$$

is given by

$$\frac{\langle c\rangle^{\beta}}{c_o} = \tfrac{1}{2}\operatorname{erfc}\left[\frac{x - \langle v_x\rangle^{\beta}t}{2\sqrt{D^{*}_{xx}t}}\right] + \tfrac{1}{2}\exp\left(\frac{\langle v_x\rangle^{\beta}x}{D^{*}_{xx}}\right)\operatorname{erfc}\left[\frac{x + \langle v_x\rangle^{\beta}t}{2\sqrt{D^{*}_{xx}t}}\right] \tag{19}$$

From measurements of the concentration as a function of time at a fixed axial position it is possible to use this relation to compute the axial dispersivity.

It is also possible to measure D^{*}_{xx} from pulses introduced into the column at $x = 0$. These pulse responses can then be analyzed by the method of moments. The Laplace transform of the solution to Eq. 16 subject to the boundary conditions of Eqs. 15 and 17 is given by

$$\overline{\langle c\rangle^{\beta}}(s) = \overline{\mathcal{F}}(s)\exp\left(\frac{\langle v_x\rangle^{\beta}x}{2D^{*}_{xx}}\right) \times \exp\left\{-x\left[\left(\frac{\langle v_x\rangle^{\beta}}{2D^{*}_{xx}}\right)^2 + \frac{s}{D^{*}_{xx}}\right]^{1/2}\right\} \tag{20}$$

The moments of the concentration response of the system at a given axial location are defined by the expression

$$m_n = \int_0^{\infty} t^n\langle c\rangle^{\beta}(x,t)dt \quad n = 0,1,2,\ldots \tag{21}$$

From a knowledge of the Laplace transform of $\langle c\rangle^{\beta}$, we can compute these moments

$$m_n = (-1)^n\frac{d^n\overline{\langle c\rangle^{\beta}}}{ds^n} \quad n = 0,1,2,\ldots \tag{22}$$

The absolute moments of $\langle c\rangle^{\beta}$ with respect to time are obtained by the simple expression

$$\mu'_n = m_n/m_o \tag{23}$$

The first absolute moment is the mean residence time for the pulse at a given axial position

$$\mu'_1(x) = m_1/m_o. \tag{24}$$

Substituting Eq. 20 in Eq. 22 with $n = 1$, we find that

$$\mu'_1(x) = \mu'_1(0) + x/\langle v_x\rangle^{\beta} \tag{25}$$

where $\mu'_1(0)$ is the mean residence time for the pulse introduced at $x = 0$. From experimental measurements of the mean residence time at a given axial position one can experimentally determine the interstitial velocity. Of course, if the bed has a uniform void fraction ϵ, this should agree with

$$\langle v_x\rangle^{\beta} = \frac{Q/A}{\epsilon} = \frac{\langle v_x\rangle}{\epsilon} \tag{26}$$

where Q is the flow rate, A the column area, and $\langle v_x\rangle$ is the superficial velocity. The second central moment $\mu_2(x)$ is a measure of the average pulse spread relative to the mean residence time

$$\mu_2(x) \equiv \frac{1}{m_o}\int_0^{\infty}(t - \mu'_1)^2\langle c\rangle^{\beta}(x,t)dt = \mu'_2 - (\mu'_1)^2 \tag{27}$$

If we substitute the expression for the Laplace transform of $\langle c\rangle^{\beta}$ into Eq. 22 and calculate m_2 and μ_2 we can show that

$$\mu_2(x) = \mu_2(0) + \frac{2D^{*}_{xx}}{x^2}[\mu'_1(x) - \mu'_1(0)]^3 \tag{28}$$

which can also be written as

$$\mu_2(x) = \mu_2(0) + 2D^{*}_{xx}\left(\frac{x}{[\langle v_x\rangle^{\beta}]^3}\right). \tag{29}$$

The quantity $\mu_2(0)$ is the spread of the pulse introduced into the column at $x = 0$. From measurements of μ_2 at various axial positions it is possible to use Eq. 29 to calculate D^{*}_{xx}, the longitudinal dispersivity, from pulse inputs into the column. Both the pulse response and the step response are convenient techniques for measuring the axial dispersivity. The accuracy of these methods will be compared in the section discussing experimental results.

The most convenient technique to measure lateral dispersivities is to consider a steady-state experiment where a uniform concentration of solute is introduced at the column entrance *distributed* over one half of the bed cross section

$$\langle c\rangle^{\beta} = \begin{cases} c_o & 0 < y < W/2 \quad \text{at } x = 0 \text{ for all } z \\ 0 & -\dfrac{W}{2} < y < 0 \end{cases} \tag{30}$$

The coordinate system is shown in Figure 1. The concentration at $x = 0$ is independent of z and as a result Eq. 6 reduces to

$$\langle v_x\rangle^{\beta}\frac{\partial\langle c\rangle^{\beta}}{\partial x} = D^{*}_{xx}\frac{\partial^2\langle c\rangle^{\beta}}{\partial x^2} + D^{*}_{yy}\frac{\partial^2\langle c\rangle^{\beta}}{\partial y^2} \tag{31}$$

In all cases considered, the concentration gradients are sufficiently steep in the y direction to neglect the dispersion contribution along the flow direction and write Eq. 31 as

$$\langle v_x\rangle^{\beta}\frac{\partial\langle c\rangle^{\beta}}{\partial x} = D^{*}_{yy}\frac{\partial^2\langle c\rangle^{\beta}}{\partial y^2} \tag{32}$$

The error caused by the neglect of the axial dispersion term is less than 1% for most values of Pe_p. Furthermore, the boundary condition in Eq. 30 can then be approximated very well by

$$\langle c\rangle^{\beta} = c_o u(y) \quad \text{at } x = 0 \tag{33}$$

where $u(y)$ is a unit step function. Eq. 32 can then be solved subject to

$$\langle c\rangle^{\beta} = 0 \quad \text{as } y \to \pm\infty \tag{34}$$

The solution is

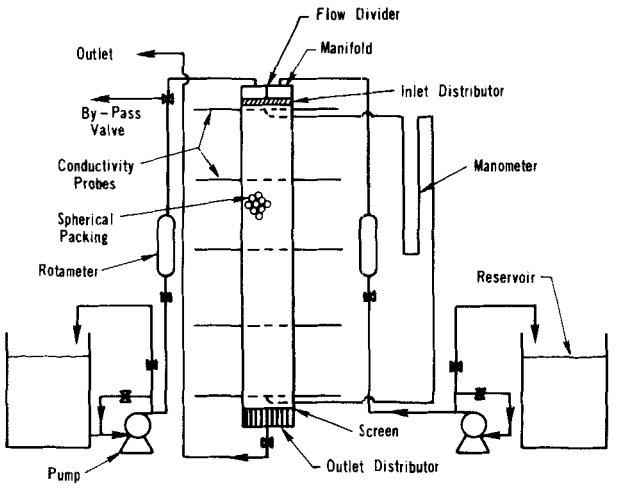

Figure 2. Overall schematic of experimental equipment.

$$\frac{\langle c\rangle^{\beta}}{c_o} = \frac{1}{2}\,\mathrm{erfc}\left\{\frac{y}{2\left(\dfrac{xD^{*}_{yy}}{\langle v_x\rangle^{\beta}}\right)^{1/2}}\right\} \tag{35}$$

and from measurements of $\langle c\rangle^{\beta}$ as a function of y we can calculate D^{*}_{yy}, the lateral dispersivity.

EXPERIMENTAL PROCEDURE

Set-Up

A plexiglas column of square cross section was constructed in order to perform the experiments outlined in the previous section and shown schematically in Figure 1. An overall diagram of the equipment is shown in Figure 2. The width W of the column is 27 cm and the height of the packing section is 150 cm. A distributor at the top insures flow uniformity. It consists of a 1.27 cm plexiglas plate with 0.32 cm diameter perforations every square centimeter. An inlet manifold 5 cm high was outfitted with a flow divider in order to perform the lateral dispersion measurements. At the outlet, a distributor consisting of 1.9 cm diameter PVC tubes 11.4 cm long insured straight streamlines at the bottom of the porous bed. Two sets of reservoirs, pumps, and rotameters were necessary in order to make the lateral dispersivity measurements.

The inlet tracer consisted of NaCl in de-ionized water at approximately 5×10^{-4} g eq./L. The molecular diffusivity of NaCl was estimated to be equal to $\mathcal{D} = 1.545 \times 10^{-5}$ cm^2/s, and the Schmidt number to be $Sc = \nu/\mathcal{D} = 560$. The density of the water which did not contain NaCl was adjusted by adding small amounts of sucrose so that it matched as well as possible

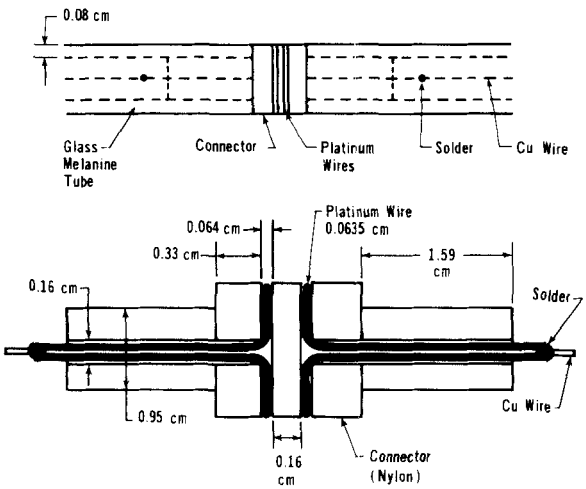

Figure 3. Platinum conductivity probe.

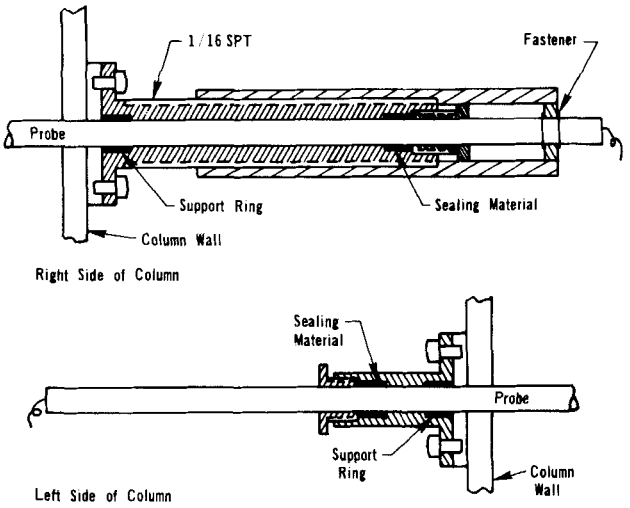

Figure 4. Device for lateral motion of probe.

the density of the NaCl solution. This helped in controlling natural convection effects at the lowest Reynolds numbers.

The concentration of NaCl was measured using the platinum conductivity probes shown in Figure 3. Platinum wires of 0.0635 cm diameter were wound in grooves on the surface of a nylon connector a distance of 0.18 cm apart. The ends of the platinum wires were soldered to copper wires which were then inserted in glass melanine tubes of 1.27 cm outer diameter. The tubes were given a thin wax coating to prevent penetration of water. The platinum rings wound around the connector were in direct contact with the fluid phase. All other portions of the wire were out of contact with the fluid since they were inserted in the platic tube. The ends of the tubes extended through the column walls and the signals were recorded on a multichannel recorder. There were five probes located in the column at the following distances from the inlet: 2.8 cm, 25.7 cm, 47.0 cm, 112.1 cm, and 147.6 cm. These probes are labeled 1 through 5, respectively. Probes 3 and 4 were designed so that they could traverse the column cross section along the y direction by means of a screw assemblage shown in Figure 4. The total moving span was 15.2 cm or about 60% of the column width. For every turn or rotation of the mechanism the probes translated a distance of 0.16 cm. As a result, it was possible to determine very accurately the probe location for the lateral concentration measurement.

The particles used in these experiments consisted of urea formaldehyde spheres of several diameters: 0.25 cm, 0.35 cm, 0.45 cm, and 0.55 cm. We also used glass spheres of 1.00 and 1.58 cm diameters. The density of the formaldehyde spheres was 1.463 g/cm^3 and those of the glass spheres was 2.94 g/cm^3 for the 1.00 cm spheres and 2.83 g/cm^3 for the 1.58 cm spheres. There was a variance of less than 0.1% from the mean particle diameter for both the glass and urea formaldehyde spheres. The void fractions were computed by carefully weighing the particles before inserting into the bed and calculating the volume of particles from the density. All the volume fractions of fluid in this experiment were in the range $\epsilon = 0.39$ to $\epsilon = 0.41$.

The column was packed by letting the particles settle in water after stirring and then tamping down slightly. The column was filled about 4 cm at a time using this procedure. Air bubbles were eliminated by degassing the water prior to use, and by carefully stirring the packing as the column was being filled.

Procedure

In the experiments for measuring the longitudinal dispersivities, both pulse inputs and step inputs were used. In the pulse input experiments the column was filled with water and drained so that the manifold above the distributor only contained about 3 mm of water. The solution containing NaCl was then carefully and slowly introduced into the manifold. The column was drained slowly so that the band of NaCl solution was introduced at the top of the packing section. The manifold was filled with water again and the pumps turned on to the desired flow rate. A recirculation or bypass line attached to the inlet line of the column was used in order to set the flow rate to the desired value prior to the start of the experiment. Once the flow rate was fixed, the fluid was diverted to the column by turning off the bypass valve and turning on the inlet line valve. This way the liquid flow rate was at the desired level throughout the length of the experiment. This

technique resulted in sharp, nearly symmetric concentration pulses at the top of the bed. The step inputs were inserted in a similar fashion by first draining the column so that only 3 mm of water was left in the manifold and then manually filling the manifold with NaCl solution. The pumps were started and the volumetric flow rate set to the desired value. The transient response at each probe was then measured using the multichannel recorder.

The lateral dispersion measurements were made by dividing the manifold into two regions by means of a 0.635 cm thick plexiglas plate. NaCl solution and water were pumped from their respective tanks, the NaCl to one side of the divider, the water to the other side. The flow rates were equalized and after a steady state was reached, the sliding probes were moved in order to measure the lateral concentration profiles. Scanning started from the fresh water side, and concentration measurements were taken every 0.16 cm, again using the recorder. After each probe displacement the system was allowed to come to a steady state prior to the concentration measurement.

Particular care was taken to ensure that the response of the probes was linear over the concentration range of 0 to 5×10^{-4} g eq./L. The circuit designed by M. Ahmon (1977) was used to process the signals from the platinum wires. Voltage was supplied to a probe only when a measurement was being taken. This was accomplished by connecting and triggering the power supply to the channel switching mechanism in the multichannel recorder. This was necessary in order to prevent stray currents between one probe and another from modifying the desired signal. We also made sure that the flow in the column was uniform by using the sliding probes. The measured responses and axial dispersion coefficients from both the step input and pulse response experiments were essentially independent of the lateral probe location, indicating a flat velocity profile and uniform inlet conditions. This was confirmed by dye observation experiments which indicated little channeling anywhere in the bed, and very small amounts of channeling near the corners. The mean residence time for the dye was identical to that for NaCl, indicating that there were no appreciable adsorption effects between the solute and the particles. This was to be expected since the ratio of bed width to mean particle diameter was about 77 in these experiments. Natural convection effects prevented us from doing experiments with particle Reynolds numbers much less than 0.3. Since we were doing experiments with relatively large particles, the Grashoff numbers were large enough to cause natural convective currents at these low liquid flow rates. This made the velocity profile in the bed nonuniform and the dispersion measurements unreliable. No runs were made with different fluid viscosities or bed diameters.

RESULTS

Longitudinal Dispersivity Measurements—Uniform Particle Size

In Figures 5 and 6 we show typical experimental results for step input and pulse response experiments when the bed was filled with particles of 0.35 cm diameter and $\epsilon = 0.41$. As can be seen, the raw data are very smooth and show little scatter for both experiments. From these time-dependent concentration measurements, Eq. 19 was used to calculate D^*_{xx} for the step input experiments and Eq. 29 was used to calculate the same quantity from the moments of the pulse response. In using Eq. 19 the value of D^*_{xx} was found from successive iterations, using the best linear fit to the inverse complementary error function of the terms in the equation. Convergence was obtained when the old and new values differd by less than 0.1%. For the case of the step input, both the velocity $\langle v_x \rangle^\beta$ and longitudinal dispersivity D^*_{xx} were treated as unknowns, and

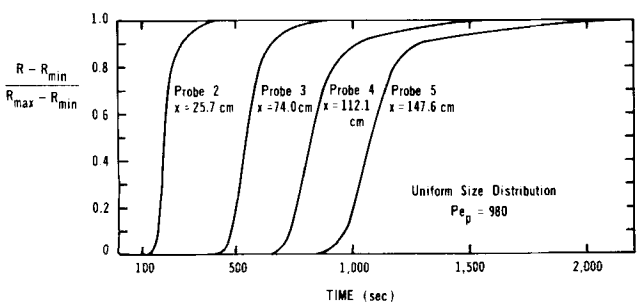

Figure 5. Sample raw data for step response experiment. *R* is recorded reading.

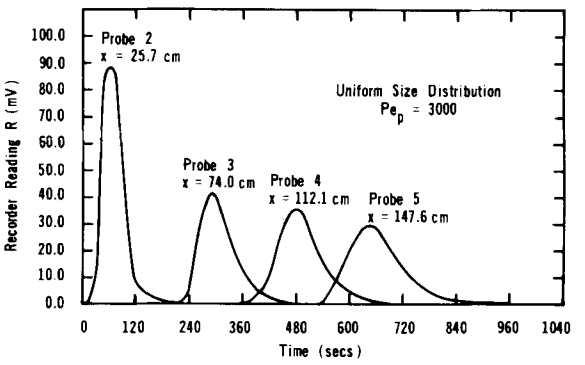

Figure 6. Sample raw data for pulse response experiment.

optimal values of these parameters were found using a search routine that analyzed the $\langle c \rangle^\beta$ versus time data at four different x values corresponding to probes 2, 3, 4, and 5. As a result, one can see variations in average fluid velocity and axial dispersivity between probe locations. Of course the true value of $\langle v_x \rangle^\beta$ is known from the overall flow rate Q, the column area A, and the true void fraction ϵ obtained from weighing the particles. One can compute an experimental volume fraction of fluid from the relation

$$\epsilon_{\text{exp}} = \frac{Q}{A \langle v_x \rangle^\beta_{\text{exp}}} \cdot \tag{36}$$

If the data and analysis are consistent, and the flow is uniform, ϵ_{exp} should closely approximate the true ϵ.

In the pulse response experiments, we computed the zeroth, first, and second moments of the time response at probes 1 through 5. The absolute first and second central moments of the response at probe 1 were treated as $\mu_1'(0)$ and $\mu_2(0)$ respectively. The value of $\mu_1'(x)$ and $\mu_2(x)$ at the remaining probe locations were used to calculate $\langle v_x \rangle^\beta$ and D^*_{xx} from Eqs. 25 and 29. An experimental void fraction can again be computed from Eq. 36.

In Figure 7 we see ϵ_{exp} as a function of Q/A, the superficial velocity for both the step and input response data. These are average void fractions between probes 2 and 5. The results compare very well with the true void fraction of 0.41, especially at large flow rates, where ϵ_{exp} is approximately 0.43. This indicates good packing and a lack of flow nonuniformities. In Figure 8 we show the longitudinal dispersivities at the various axial locations as a function of the Peclet number obtained from the pulse response experiments. These data exhibit a great deal of scatter due to the inaccuracies of calculating the second moments of the experimental data. Small differences in the way the tails of the concentration response are truncated and small errors in the value of measured concentration for very low values of concentrations give extremely large errors in computed D^*_{xx}. This factor contributes significantly to the large amount of scatter found in dispersion data. In contrast, Figure 9 shows the results for axial dispersivities using the step response data. It is clearly much less scattered, and it shows clear

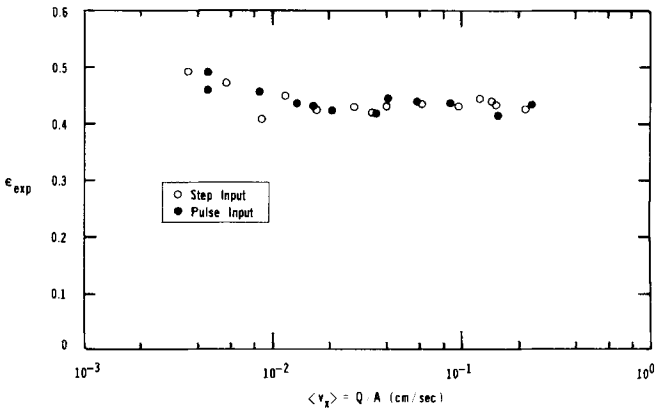

Figure 7. Volume fractions obtained from probe response.

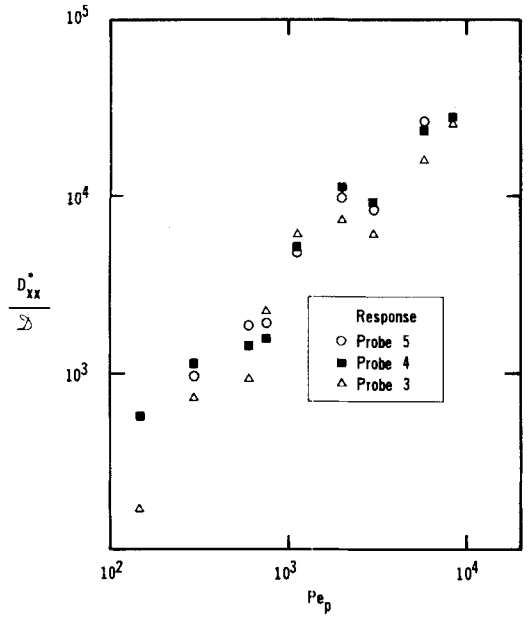

Figure 8. Longitudinal dispersivities from pulse response experiments—uniform particles.

trends of the variation of the longitudinal dispersivity with Peclet number and probe location. We note from Figure 9 that for $Pe_p < 10^3$ the values of D^*_{xx} are nearly identical for all values of $x = L$, or probe location. However, as the Peclet number nears 10^4 one begins to notice a significant difference between the dispersion coefficient calculated at 25.7 cm and that computed at 147.6 cm. Basically, one can observe an increase in the value of the dispersion coefficient with increasing distance down the column. The larger the value of the Peclet number, the larger the discrepancy between the dispersion coefficient measured at $x = 25.7$ cm and $x = 147.6$ cm.

In Eq. 2 we have expressed the time criterion required in order to obtain a constant value of the longitudinal dispersivity. If we associate with time t since injection of the pulse the quantity $L/\langle v_x \rangle^\beta$, and substitute the characteristic length l_β defined in Eq. 3, we can rewrite the time constraint in Eq. 2 as

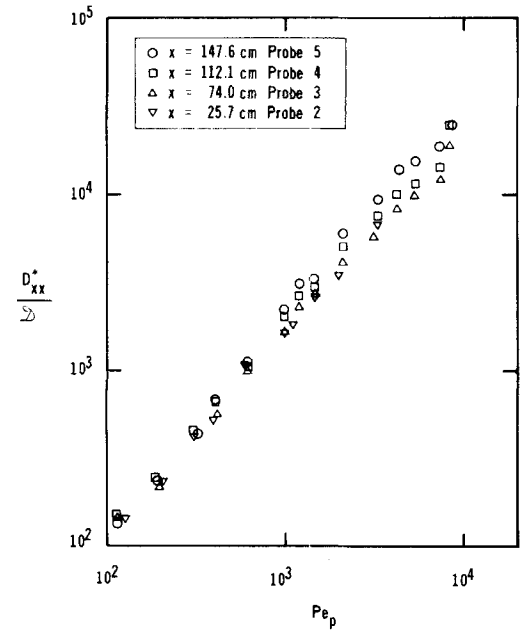

Figure 9. Longitudinal dispersivities from step response experiments—uniform particles.

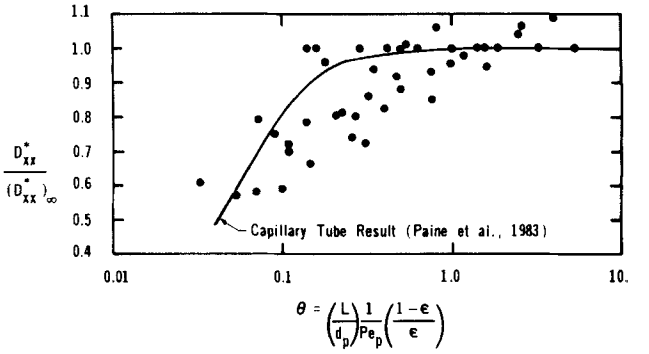

Figure 10. Longitudinal dispersivity dependence on θ.

$$\theta = \left(\frac{L}{d_p}\right)\frac{1}{Pe_p}\left(\frac{1-\epsilon}{\epsilon}\right) \gg 1. \tag{37}$$

We can develop a quantitative criterion for when the axial dispersivity is constant by taking the axial dispersivities shown in Figure 9 at the probe locations 2, 3, and 4, and dividing them by the dispersivity measured at location 5 at each Peclet number $(D^*_{xx})_\infty$. Since L is different at the different probes, we can compute θ for each probe according to Eq. 37. The results are shown in Figure 10 for all Peclet numbers $Pe_p \leq 5 \times 10^3$. We did not carry out the data analysis for higher Peclet numbers since for these high Peclet numbers it is possible that we have not achieved the final value of D^*_{xx} even at the last probe location. For values of $\theta > 1$, the ratio of D^*_{xx} to $(D^*_{xx})_\infty$ oscillates about 1.0 with about a 10% variation. This is a good measure of the accuracy of the experiment. We see that for $\theta \geq 0.3$, one can be assured of being within 90% of the final constant value of the longitudinal dispersivity. We can conclude that Eq. 37 is too restrictive, and in fact one can expect constant longitudinal dispersivities as long as

$$\theta = \left(\frac{L}{d_p}\right)\frac{1}{Pe_p}\left(\frac{1-\epsilon}{\epsilon}\right) \geq 0.3 \tag{38}$$

This is the constraint that should be considered when requiring constant longitudinal dispersivities in a transient axial dispersion experiment. In Figure 10 we also show the theoretical prediction of Paine et al. (1983) on the time dependence of the axial dispersion coefficient. Even though this calculation was done for a capillary tube, one can see a very similar trend to that shown by the data.

In Figure 11 we compare our data for probe 5, the largest dispersion distance, to a great deal of axial dispersion data in the literature, mostly from references listed in Table 1. There is a very good agreement between our results and previous values even though our data tend to be on the lower side of the previously published results. We believe this is due to the fact that we have taken great pains to reduce effects due to particle size distributions,

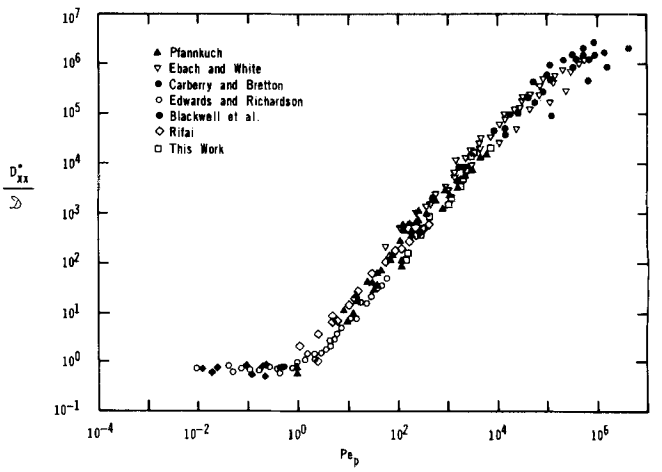

Figure 11. Longitudinal dispersivity values from various experiments.

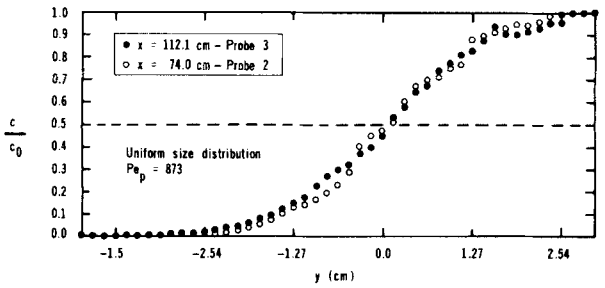

Figure 12. Sample raw data from lateral dispersion experiments.

small ratios of column-to-particle diameter, flow nonuniformities, and natural convection induced by density differences. One can see a curvature of the collected data at Peclet numbers greater than 10^4. Bear (1972) has ascribed this to turbulence effects in the porous media. However, note that the two experiments that exhibit this curvature at high Peclet number are those of Carberry and Bretton (1958) and Ebach and White (1958) where the constraint of Eq. 4 is violated. In Figure 9 we show curvature of the dispersion data with Peclet number when the column length does not satisfy the criterion of Eq. 4. The results of our work are not explainable in terms of turbulence since the highest Reynolds numbers we used were on the order of 18. This is far below the laminar-to-turbulent transition in packed bed studies. Careful analysis of the data in Figure 11 indicates that there is curvature also in the data of Pfannkuch (1963) where Table 1 indicates that the criterion of Eq. 4 is marginally satisfied and the Reynolds numbers are no higher than 10.

This is very convincing evidence that the curvature seen in Figure 11 is not dependent on turbulent effects, but simply too short a column for the high flow rates used. As Figure 10 indicates, if the column is too short one can measure a dispersion coefficient that is significantly lower than the final asymptotic value.

Lateral Dispersivity Measurements—Uniform Particle Size

In Figure 12 we show a typical plot of the lateral concentration profiles measured during steady-state experiments aimed at determining the lateral dispersivities. There is an increase in the spread of the concentration profile from $x = 74.0$ cm to $x = 112.1$ cm. Equation 35 was used to calculate D^*_{yy} from known values of $\langle v_x \rangle^\beta$ and x, and the concentration profile. This was accomplished by plotting the inverse complementary error function of $2\langle c_x \rangle^\beta / c_o$ as a function of y and finding the slope (Harleman and Rumer, 1963). The results are shown in Figure 13, together with some collected values from the literature. The results are independent of probe location. We have plotted in Figure 13 all of the data taken at both probes. Previous results for lateral dispersivities had covered the Peclet number range from 10^{-1} to 10^3. Our data extend the available values up to a Peclet number of 10^4. As can be seen from Figure 13 there is very good agreement between our results and those of Harleman and Rumer (1963) in the Peclet number range where they overlap.

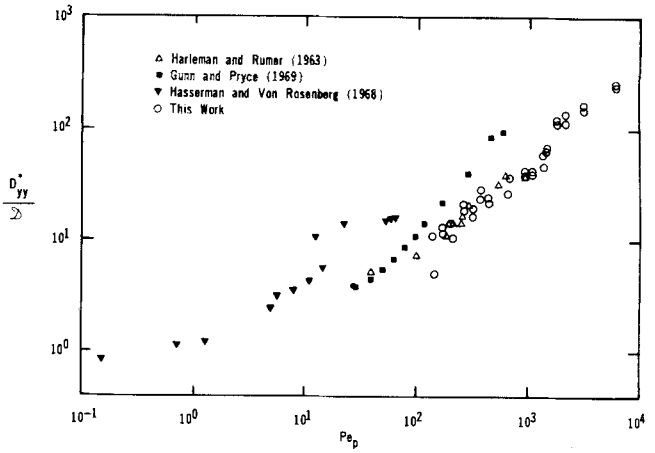

Figure 13. Lateral dispersivity values from various experiments.

Effect of Particle Size Distribution on Longitudinal and Lateral Dispersion

In order to study the effect of the distribution of particle sizes on longitudinal and lateral dispersion coefficients, we repeated the measurements described above for two different particle size distributions that had the same void fraction and the same mean particle diameter, but different particle size ranges. Details of the particles that made up these distributions are given in Table 2. Size distribution 1 has $\epsilon = 0.39$ and a mean particle diameter $\bar{d}_p$ of 0.35 cm. Size distribution 2 has $\epsilon = 0.41$ and the identical value of $\bar{d}_p$. This is the same diameter as the particle size used in the experiments described previously in which all the particles had a uniform size. The mean particle diameter is defined as

$$\bar{d}_p = 6\frac{V_p}{A_p} = \sum_i n_i d_{pi}^3 \Big/ \sum_i n_i d_{pi}^2 \tag{39}$$

where V_p and A_p are the total volume and surface area of the particles in the bed, n_i is the number fraction, and d_{pi} is the diameter of each size particle. Equation 39 can be rewritten using the weight fractions and densities of the different particles

$$\bar{d}_p = \sum_i (x_i/\rho_i) \Big/ \sum_i (x_i/\rho_i d_{pi}). \tag{40}$$

This is the most convenient way to compute $\bar{d}_p$ from measured weights of each type of particle. The main difference between size distributions 1 and 2 is that size distribution 2 has a small percentage of very large particles where the ratio of maximum to minimum particle diameter is 7.3. Size distribution 1 has a ratio of maximum to minimum particle diameter of 2.2. Even though the large particles in size distribution 2 are only a very small fraction of the total number, they make up about 11% of the total volume.

Longitudinal Dispersion

In Figure 14 we show the values of $D^*_{xx}/\mathcal{D}$ measured at different probe locations using step input experiments for the case of a uni-

TABLE 2. PARTICLE SIZE DISTRIBUTION

Distribution 1 ($\epsilon = 0.39$, $\bar{d}_p = 0.35$ cm)						
Particle type,* i	1	2	3	4	5	6
Particle diameter d_{pi} (cm)	0.25	0.35	0.45	0.55	1.00	1.58
Number fraction n_i	0.649	0.237	0.074	0.040	—	—
Weight fraction x_i	0.30	0.30	0.20	0.20	—	—
Volume fraction v_i	0.30	0.30	0.20	0.20	—	—
Distribution 2 ($\epsilon = 0.41$, $\bar{d}_p = 0.35$ cm)						
Particle type,* i	1	2	3	4	5	6
Particle diameter d_{pi} (cm)	0.25	0.35	0.45	0.55	1.00	1.58
Number fraction n_i	0.6604	0.2808	0.0566	—	0.0017	0.00045
Weight fraction x_i	0.30	0.35	0.15	—	0.10	0.10
Volume fraction v_i	0.3328	0.3882	0.1665	—	0.0552	0.0573

*Particle types 1–4 are urea formaldehyde spheres, $\rho_i = 1.463$ g/cm^3.
Particle types 5–6 are glass spheres $\rho_5 = 2.940$ g/cm^3, $\rho_6 = 2.83$ g/cm^3.

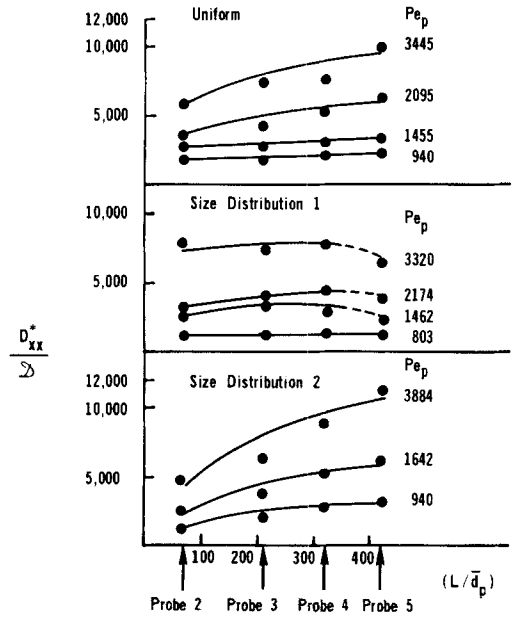

Figure 14. Effect of particle size distribution on longitudinal dispersivity at various probe locations.

form particle size, size distribution 1, and size distribution 2 for representative Peclet numbers. We note that for size distribution 1 and the uniform particle size case, the longitudinal dispersivity values become constant at shorter dispersion lengths than for the wider size distribution 2. For example, it is not clear that the asymptotic value of $D^*_{xx}/\mathcal{D}$ has been reached at a Peclet number of 1,642 in size distribution 2. However, for the uniform particles and size distribution 1 one sees nearly constant values of longitudinal dispersivities at Pe_p = 1,455 and 1,462 respectively. It is apparent that the wider size distribution has a longer characteristic length than that used in Eq. 3. One can conjecture that this is due to a larger scale nonuniformity in the macroscopic flow field, but there are not enough data at this time to quantify the effect. Mention should be made of the apparent slight decrease in the longitudinal dispersivity found at the last probe in the experiments with size distribution 1. We believe this is an artifact in the experiment caused by either a slight bending of the probe or a packing nonuniformity near the electrode. This phenomenon was not observed in either of the other two packings.

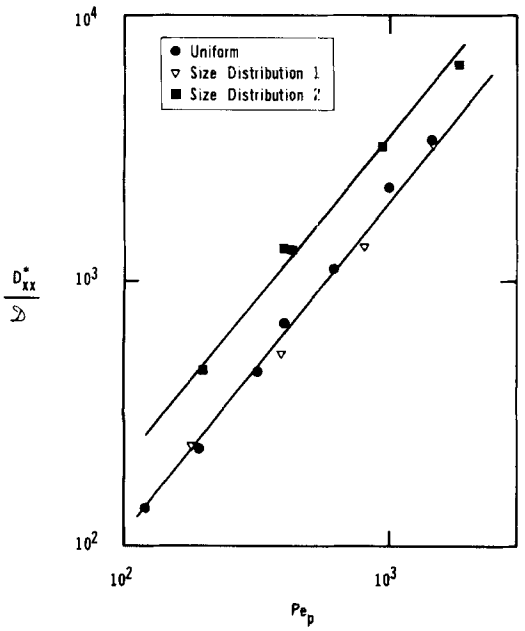

Figure 15. Longitudinal dispersivities for uniform particles, size distribution 1 and size distribution 2.

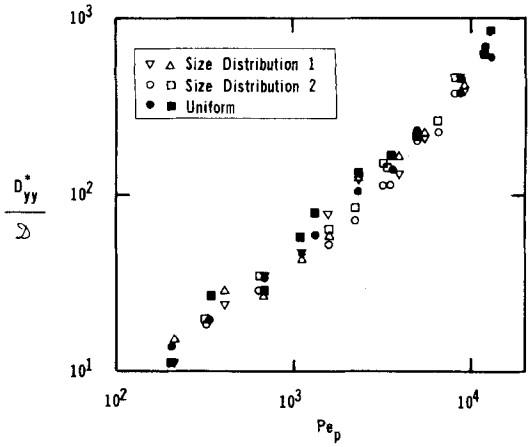

Figure 16. Effect of particle size distribution on lateral dispersivities.

Since size distribution 2 showed a larger required length to achieve constant axial dispersivities, we need to be a little careful in deciding which are the final asymptotic longitudinal dispersivities measured for this size distribution. Figure 14 indicates that for a Pe_p for 1,642 or less, the longitudinal dispersivity measured at probe 5 is fairly close to its final value. In comparing the results for the three different size distributions we chose only those particle Peclet numbers less than 2,000. This way we are more or less assured of comparing longitudinal dispersivities which have reached their final value at a particular particle Peclet number. In Figure 15 we have plotted the highest values of $D^*_{xx}/\mathcal{D}$ measured for the three size distributions for this small Peclet number range. Note that there is almost no difference at all between the results for the case of uniform packing and size distribution 1. Since the mean particle sizes are the same, the volume fraction is nearly the same, and the ratio of maximum to minimum size is not too far from 1, one does not observe much of a difference between size distribution 1 and the uniform case. However, the values of $D^*_{xx}/\mathcal{D}$ for size distribution 2 are larger by a significant amount (about a factor of 2) than those for the uniform particle size case. The two lines of data are nearly parallel, indicating that one could superimpose them if there was a re-definition of the characteristic length in the Peclet number for the case of wide particle size distributions. This is consistent with the results of Figure 14, which also indicated that there was a length scale, larger than the mean hydraulic radius, which dominates the approach to a constant axial dispersivity value.

It should be noted that the three different packings used—the uniform particles and size distributions 1 and 2—have nearly identical hydraulic radii since they have the same value of $\bar{d}_p$ and nearly the same volume fraction. As a result, the observed differences in longitudinal dispersivities must be caused by the spread of the size distribution alone. Eidsath et al. (1983) computed longitudinal dispersivities in two dimensional spatially periodic arrays of cylinders with two different radii. They found that when the ratio of cylinder radii was increased from 2 to 5, the axial dispersivity increased by a factor of 1.5 at the same Peclet number. This is an increase of the same order as was found in the experimental observations presented in this work. Carbonell (1979) also found a very strong dependence of longitudinal dispersivities on the spread of pore size distributions for a very simple capillary tube model of the porous medium. If one is willing to associate an increased particle size distribution with an increased pore size distribution, the trend observed in the experiments just described is at least qualitatively the same as that predicted by the theory. Additional experiments need to be done before this effect can be understood fully, but it is clear that one needs to emphasize the role of the width of the particle size distribution on the dispersion process.

Lateral Dispersion

In Figure 16 we have collected the results for lateral dispersivities D^*_{yy} for the uniform particle size case, as well as for size distributions 1 and 2. There is no evidence to indicate a change in the lateral dispersion with particle size distribution. At least, lateral dispersivities seem to be much less sensitive to size distribution than longitudinal dispersivities. This conclusion perhaps should be qualified by the fact that we took steady-state measurements of D^*_{yy}. One should expect that D^*_{yy} values measured in a transient experiment would be subject to the same long-time constraint as the longitudinal dispersivities. There have been only one theoretical estimate of the effect of particle size distribution on lateral dispersion. Eidsath et al. (1983) found that when the ratio of cylinder radii in a two-dimensional spatially periodic array was changed from 2 to 5, the lateral dispersivity actually decreased by a factor of about 3, but this is an artifact of the extremely simple geometry employed in these computations.

ACKNOWLEDGEMENT

This work was supported by NSF Grant ENG. 7913269.

NOTATION

$A_{\beta\sigma}$ = fluid-solid interfacial area
A = column cross sectional area
A_p = total surface area of particles in bed
c = point solute concentration
c_o = solute concentration in input
$\tilde{c}$ = spatial deviation in solute concentration
$\langle c\rangle^\beta$ = interstitial average solute concentration
$\overline{\langle c\rangle^\beta}$ = Laplace transform of $\langle c\rangle^\beta$
d_p = particle diameter
$\overline{d_p}$ = average particle diameter
d_{pi} = diameter of particles of type i
$\boldsymbol{D}$ = hydrodynamic dispersion tensor
$\boldsymbol{D}^*$ = total dispersivity tensor
D^*_{xx}, D^*_{yy} = longitudinal and lateral dispersivities
$\mathcal{D}$ = molecular diffusivity
f = closure function for the spatial deviations
$\mathcal{I}(t)$ = time-dependent inlet concentrations
$\overline{\mathcal{I}}(s)$ = Laplace transform of $\mathcal{I}$
$\boldsymbol{I}$ = unit tensor
l_β = characteristic length for fluid between particles
L_C = characteristic length for average concentration changes
m_n = nth moment of the average concentration with time
n_i = number fraction of particle type i
$\boldsymbol{n}$ = unit normal from fluid to solid
Pe_p = particle Peclet number
Q = volumetric flow rate
R = capillary tube radius
r_o = radius of the averaging volume
R_p = particle Reynolds number
s = Laplace transform variable
Sc = Schmidt number
t = time
$u(t), u(y)$ = unit step functions in time and lateral position
v = point velocity vector in fluid phase
$\tilde{v}$ = spatial deviation in fluid velocity
$\langle v\rangle^\beta$ = interstitial average velocity vector
$\langle v_x\rangle, \langle v_x\rangle^\beta$ = superficial and interstitial average velocity in flow direction
v_i = volume fraction of particle type i
V_p = total volume of particles in bed
W = width of bed
x = axial position in bed
x_i = weight fraction
y = Cartesian coordinate normal to flow direction
z = Cartesian coordinate normal to flow direction
$\langle\ \rangle^\beta$ = refers to an interstitial average

Greek Letters

ϵ = void fraction
ρ_i = density of particle of type i
τ = tortuosity tensor
μ'_n = nth absolute moment in time
μ_n = nth central moment in time
ν = kinematic viscosity
β = refers to the fluid phase

LITERATURE CITED

Ahmon, M., "One-Chip Conductivity Meter Monitors Salt Concentrations," *Electronics*, 132 (Sept. 15, 1977).

Aris, R., "On the Dispersion of a Solute in a Fluid Flowing through a Tube," *Proc. Roy. Soc.* **A235,** 67, London (1956).

Bear, J., *Dynamics of Fluids in Porous Media*, Elsevier Pub. Co., New York (1972).

Blackwell, R. J., J. R. Rayne, and W. M. Terry, "Factors Influencing the Efficiency of Miscible Displacement," *AIME Petroleum Trans.*, **217,** 1 (1959).

Blackwell, R. J., "Laboratory Studies of Microscopic Dispersion Phenomena," *Soc. Petroleum Eng. J.*, 1 (Mar., 1962).

Brenner, H., "Dispersion Resulting from Flow through Spatially Periodic Porous Media," *Phil. Trans. Roy. Soc.*, **297,** 81, London (1980).

Carberry, J. J., and R. H. Bretton, "Axial Dispersion of Mass in Flow through Fixed Beds," *AIChE J.*, **4,** 367 (1958).

Carbonell, R. G., "Effect of Pore Size Distribution and Flow Segregation on Dispersion in Porous Media," *Chem. Engr. Sci.*, **34,** 1,031 (1979).

———, "Flow Non-Uniformities in Packed Beds: Effect on Dispersion," *Chem. Engr. Sci.*, **35,** 1,397 (1980a).

———, "Effect of Particle Size Distribution and Flow Non-Uniformities on Dispersion in Porous Media: Application to Oil Shale Retorts," *Proc. 2nd Multiphase Flow and Heat Transfer Symp.*, T. Veziroglu, Ed., 2379 (1980b).

Carbonell, R. G. and S. Whitaker, "Dispersion in Pulsed Systems. Part II: Theoretical Developments for Passive Dispersion in Porous Media," *Chem. Eng. Sci.*, **38,** 1795 (1983).

De Josselin de Jong, G., "Longitudinal and Transverse Diffusion in Granular Deposits," *Trans. Amer. Geophys. Union*, **39,** 67 (1958).

Dullien, F. A. L., *Porous Media: Fluid Transport and Pore Structure*, Academic Press, New York (1979).

Ebach, E. A., and R. R. White, "Mixing of Fluids Flowing through Beds of Packed Solids," *AIChE J.*, **4,** 161 (1958).

Eidsath, A., et al., "Dispersion in Pulsed Systems. Part III: Comparison between Theory and Experiments for Packed Beds," *Chem. Engr. Sci.*, **38,** 1803 (1983).

Edwards, M. F., and J. F. Richardson, "Gas Dispersion in Packed Beds," *Chem. Engr. Sci.*, **23,** 109 (1968).

Gill, W. N., and R. Sankarasubramanian, "Exact Analysis of Unsteady Convective Diffusion", *Proc. Roy. Soc.* **A316,** 341, London (1970).

Grane, F. E. and G. H. F. Gardner, "Measurements of Transverse Dispersion in Granular Media," *J. Chem. Eng. Data*, **6,** 283 (1961).

Gray, W. G., "A Derivation of the Equations for Multiphase Transport," *Chem. Engr. Sci.*, **30,** 229 (1975).

Greenkorn, R. A., and D. P. Kessler, "Dispersion in Heterogeneous, Non-Uniform, Anisotropic Porous Media," *Flow Through Porous Media*, Amer. Chem. Soc., Washington, D.C. (1970).

Gunn, D. J., and C. Pryce, "Dispersion in Packed Beds," *Trans. Inst. Chem. Eng.*, **47,** T341 (1969).

Haring, R. E., and R. A. Greenkorn, "A Statistical Model of a Porous Medium with Non-Uniform Pores," *AIChE J.*, **16,** 477 (1970).

Harleman, D. R. F., and R. R. Rumer, "Longitudinal and Lateral Dispersion in an Isotropic Porous Medium," *J. Fluid Mech.*, **16,** 385 (1963).

Hassinger, R. C., and D. U. von Rosenberg, "A Mathematical and Experimental Examination of Transverse Dispersion Coefficients," *Trans. Soc. Petroleum Eng. J.*, **243,** 195 (1968).

Niemann, E. H., "Dispersion during Flow in Non-Uniform Heterogeneous

Porous Media", MS Thesis, Chem. Eng. Dept., Purdue Univ., Lafayette, IN (1969).
Paine, M. A., R. G. Carbonell, and S. Whitaker, "Dispersion in Pulsed Systems. Part I: Heterogeneous Reaction and Reversible Adsorption in a Capillary Tube," *Chem. Eng. Sci.*, **38**, 1781 (1983).
Pfannkuch, H.-O., "Contribution à l'Etude des Déplacements des Fluides Miscibles dans un Milieu Poreux," *Revue de l'Institut du Pétrole*, **18**, 215 (1963).
Rifai, M. N. E., W. J. Kaufman, and D. K. Todd, "Dispersion in Laminar Flow through Porous Media", *Sanitary Eng. Res. Lab. Rpt. No. 3, IER Series* **90**, Berkeley, CA (July 1, 1956).
Ryan, D., R. G. Carbonell, and S. Whitaker, "A Theory of Diffusion and Reaction in Porous Media," *AIChE Symp. Ser., No. 202*, **77**, 46 (1981).
Saffman, P. G., "Dispersion in Flow through a Network of Capillaries," *Chem. Eng. Sci.*, **11**, 123 (1959).
Slattery, J. C., *Momentum, Energy, and Mass Transfer in Continua*, McGraw-Hill, New York (1972).
Taylor, G. I., "Dispersion of Soluble Matter in Solvent Flowing Slowly through a Tube," *Proc. Roy. Soc.*, **A219**, 186, London (1953).
——, "Conditions under Which Dispersion of a Solute in a Stream of Solvent Can be Used to Measure Molecular Diffusion," *Proc. Roy. Soc.*, **A225**, 473, London (1954).
Whitaker, S., "Diffusion and Dispersion in Porous Media," *AIChE J.*, **13**, 420 (1967).
Whitaker, S., "Forced Convection Heat Transfer Correlations for Flow in Pipes, Past Flat Plates, Single Cylinders, Single Spheres, and for Flow in Packed Beds and Tube Bundles," *AIChE J.*, **18**, 361 (1972).

Manuscript received April 11, 1983; revision received November 15, 1983, and accepted December 7, 1983.

Particle Collection in Magnetically Stabilized Fluidized Filters

A study was conducted on the use of magnetically stabilized fluidized (MSF) filters for removing fine particles from gases. The effect on filter performance of a number of variables was examined, including the applied field strength, gas velocities, and bed height. The dynamic behavior of MSF filters was found to be characterized by a decreasing collection efficiency with time as a result of significant particle re-entrainment.

R. V. ALBERT and CHI TIEN

Department of Chemical Engineering and Materials Science
Syracuse University
Syracuse, NY 13210

SCOPE

Granular filtration has been applied extensively in the past to control particulate emission and has proven effective for particles with a wide size range. It is particularly suitable for operation under high temperature and pressure conditions. On the other hand, granular filtration is inherently unsteady state. The accumulation of fine particles within a filter requires periodic media regeneration.

A possible way of overcoming the shortcomings arising from the cyclic nature of granular filtration is to operate filter beds in the fluidized mode, thus allowing a continuous withdrawal and introduction of filter grains. Furthermore, if fluidization is carried out with magnetic stabilization, the presence of gas bubbles in the bed can be eliminated and/or reduced. One may speculate that such an arrangement offers an ideal combination of high collection efficiency of granular filtration and the advantage of continuous operation, which is desirable in large-scale applications.

This paper reports results obtained from a systematic experimental study of the performance of magnetically stabilized fluidized (MSF) filters. The effect on filter performance of a number of variables was examined, including the magnetic field strength, gas velocities, bed height, and the size of fluidized particles. Experiments were also conducted on the extent of particle re-entrainment.

The concept of the unit collector efficiency proposed by Tien and Payatakes (1979) was used to assess the effectiveness of MSF filters and as a basis for comparing the performance of a MSF filter with its equivalent fixed-bed filter. The feasibility of employing a phenomenological rate expression to describe the dynamic behavior of MSF filters was also demonstrated.

CONCLUSIONS AND SIGNIFICANCE

The results of this experimental study demonstrate that substantial particle collection efficiency over long operating periods can be achieved with the use of fluidized filters under magnetic stabilization.

Compared with fixed-bed filters of comparable bed height, MSF filters give a somewhat lower collection efficiency. The most important variable affecting the performance of MSF filters is the applied magnetic field strength. Another important finding is the significant particle re-entrainment that occurs as the specific deposit of the filter increases. As a result, MSF filters, in most cases, exhibit a decrease in collection efficiency with time.

The dynamic behavior of MSF filters can be approximately described by the phenomenological equation for deep-bed filtration with the inclusion of particle re-entrainment.